SINERGI Vol. 28, No. 1, February 2024: 141-152
http://publikasi.mercubuana.ac.id/index.php/sinergi
http://doi.org/10.22441/sinergi.2024.1.014

Resonance analysis of fan blade design using Finite Element Method

Dedik Romahadi[1,2,*], Rikko Putra Youlia[1], Himawan S. Wibisono[1], Muhammad Imran[3]
[1]Department of Mechanical Engineering, Faculty of Engineering, Universitas Mercu Buana, Indonesia
[2]School of Mechanical Engineering, Beijing Institute of Technology, China
[3]School of Material Science and Technology, Beijing Institute of Technology, China

Abstract
Fan motors move liquids, such as air, in the gas phase from one place to another. The frequency of the fan blades, which are the main components of the fan motor, can vary. It is crucial to know the frequencies of each fan blade to avoid design failures caused by resonance. This research analyzes the effect of differences in the angle and number of blades on the natural frequency of the fan to avoid resonance with the motor rotation frequency. Modeling and simulation using the finite element method in the Solidworks application are used to determine the natural frequencies of the fan. Fans come in various configurations, with blades ranging from two to four, and blade pitch can be 25°, 30°, or 40°. Variations in the number of fan blades and changes in blade pitch show that the low mode shape does not affect the natural frequency, while the high mode has a negligible effect. The natural frequency of fan blades 2, 3, and 4 exhibits variations when operated with motors running at 25, 35, or 50 Hz. The findings imply that the fan blades' inherent frequency does not align closely with the motor rotational frequency, indicating that the design is safe.

This is an open-access article under the CC BY-SA license

Keywords:
Blade Fan;
Resonance;
Natural Frequency;
FEM

Article History:
Received: July 27, 2023
Revised: November 22, 2023
Accepted: November 30, 2023
Published: February 2, 2024

Corresponding Author:
Dedik Romahadi
Mechanical Engineering Department, Universitas Mercu Buana, Indonesia
School of Mechanical Engineering, Beijing Institute of Technology, China.
Email: dedik.romahadi@mercubuana.ac.id

INTRODUCTION

The fan is a system with mass and elasticity that can experience vibrations when subjected to disturbances [1][2]. The disturbance can come from the system (free vibration) or be caused by external influences (forced vibration). Due to the large and elastic properties of the material, as well as the disturbance or excitability, the fan-like machine structure is a vibration system [3][4]. Vibration frequency is the number of vibrations the system makes in one second or the number of vibration periods at one time [5]. A resonance state occurs when the excitation force's frequency coincides with one of the system's natural frequencies. Increasing the system's natural frequency creates significant vibrations [6][7]. Determining the natural frequencies is of utmost importance in a system subject to vibration. From rotating machine modules, motion analysis software using the finite element approach can build and simulate unbalanced models. Up-down models and graphs can be created using the Solidworks application [8, 9, 10], for instance, a model of a spinning machine and a diagram showing its acceleration with time. Using the finite element method, a module of a rotating device can be simulated, resulting in several modes. At 1280 rpm, the rotary engine module deviation is projected into the fifth mode. The rotary machine module's operating frequency must differ from the natural frequency anticipated using finite elements. The 1280 rpm figure is still above the natural frequency and will not cause mutually reinforcing vibrations to make the module construction safe [11, 12, 13].

The natural frequency, called the eigenfrequency, denotes the frequency at which a system oscillates without any external driving force. The natural frequency of the fan blade is

determined by the specific characteristics of its geometry and material composition [14, 15, 16]. The equation of motion for the Vehicle Manipulator was derived from the modeling process, as depicted in Figure 1. A significant fan vibration load increases when the blade's natural frequency coincides with the fan component's primary frequency. Hence, it is preferable to prevent the blade's natural frequency from coinciding with the dominant frequency of the fan component to decrease the risk of fan design failure.

Resonance is a phenomenon that occurs when an oscillating system is affected by a series of periodic pulses that are the same or nearly the same as one of the natural frequencies of the system's oscillations. The system will oscillate with relatively large or maximum amplitude [17][18]. Resonance must sometimes be suppressed in everyday life. Otherwise, it can lead to danger or disaster. Similar to the abovementioned incident, another Tacoma Strait suspension bridge collapse occurred in the United States in 1940. The wind blowing through the bridge at a certain speed and frequency also creates resonance in the bridge. The bridge began to sway aggressively, eventually collapsing [19, 20, 21].

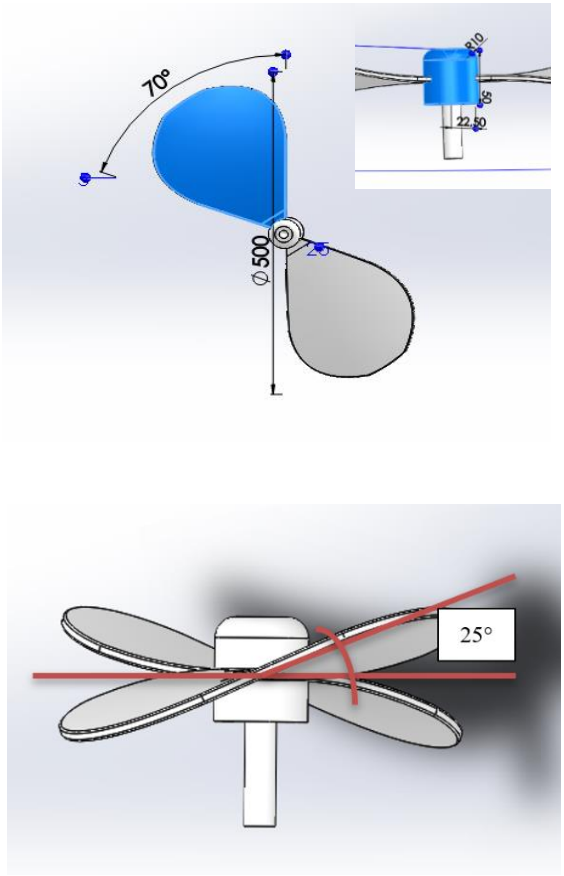

Figure 1. Number of blades 2 and 25°

Using the finite element method, it is possible to translate fan vibrations using rigorous mathematical calculations. The finite element approach is a computer-based procedure for analyzing continuous structures and materials. This strategy is based on building complex objects with a small number of simple bricks or reducing complex things into small, manageable pieces [22, 23, 24]. The finite element method uses a numerical method to solve the boundary value problem characterized by partial differential equations and boundary conditions. Vibration analysis is a method that has been effectively used to detect the initial damage that occurs to a machine, especially to detect the location of the damage [25][26].

In this study, the authors would like to add references related to resonance in structural vibration [27]. The mitigation strategies employed to minimize structural vibration can be categorized into three main approaches: vibration source damping, propagation damping, and structural vibration reduction [28][29]. Some researchers proposed a set of recommendations aimed at mitigating floor vibration issues caused by external disturbances, drawing from their analysis of various case studies encompassing office buildings and resonance. The motor's speed can be decreased using a frequency converter or a gearbox to reduce vibration in power equipment. This ensures that the operating frequency of the engine does not coincide with the structure's natural frequency, avoiding resonance [30]. In the context of a coal conveying tower project, it was observed that significant vibrations were present within the tower during motor operation. This phenomenon can be attributed to the proximity of the vertical vibration frequencies shown by both the motor and the floor, leading to a state of resonance. Following the adjustment of the motor frequency, it was observed that the vibration phenomenon exhibited a significant reduction. One approach to mitigating transmission path vibration involves implementing vibration isolation ditches or piles between the structure and the external vibration source. This impedes the propagation of waves the vibration source generates toward the building [31, 32, 33]. Measures aimed at reducing structural vibrations encompass various strategies. These strategies may involve enhancing the foundation's stiffness or implementing floating slabs to mitigate the transmission of vibrations to the structure's interior. Additionally, installing steel braces between columns or incorporating shear walls can be employed to reinforce the lateral stiffness of industrial factory buildings [34].

In this study, variations in the angle and number of fan blades for natural frequencies will be studied using Solidworks's finite element method to identify the magnitude of the effect on the modifications made and to prevent resonance with the motor rotation.

METHOD

Designing fan blades starts with creating a 3D model using Solidworks with several models of varying blade pitch and the number of fan blades. This process must be done carefully so that errors do not occur when the analysis does not occur. Simulating an image of a fan blade and analyzing its natural frequency with the finite element analysis (FEA) method on Solidworks until the data results are released. This FEA analysis was carried out numerically to get the desired results with variations in the angle of the blades and the number of edges. If the FEA simulation and analysis run, it can proceed to the following process. However, suppose there is a failure in the Solidworks simulation and FEA analysis process. In that case, it returns to changing the geometry of the 3D model until the frequency analysis is finally successfully carried out. Each design variation will be compared with its frequency value. Selection of the best design in terms of the difference in the value of the frequency of the fan blades with the motor. The analysis process goes through several stages that must be carried out, namely, setting the analysis parameters, creating a mesh, running the analysis, and determining the results of the research. The last step is to analyze the natural frequency result data obtained from Solidworks to get the desired results.

FEM-Based Method for Modal Analysis

The objective of modal analysis in structural mechanics is to ascertain an object or structure's inherent mode shapes and frequencies when undergoing unforced oscillation. The utilization of the finite element method (FEM) for conducting this study is prevalent due to its ability to handle objects with any shape and produce satisfactory calculation outcomes, similar to other FEM-based computations. The equations encountered in modal analysis are the same as those found in eigensystems. The eigenvalues and eigenvectors obtained from solving the system can be interpreted physically as representing the frequencies and related mode shapes. Sometimes, the sole preferred vibration modes are those characterized by the lowest frequencies. This preference arises from these modes exhibiting an object's most pronounced vibrational behavior, hence overshadowing any higher-frequency modes [35].

Additionally, it is feasible to conduct a physical examination of an object to ascertain its inherent frequencies and mode shapes. The term used to describe this process is Experimental Modal Analysis. The outcomes of the physical examination can be employed to align a finite element model with ascertaining the accuracy of the underlying assumptions, such as utilizing appropriate material attributes and boundary conditions. The matrix equations for a fundamental problem concerning a linear elastic material that adheres to Hooke's Law can be represented as a dynamic system of spring masses in three dimensions [36][37]. The equation representing the generic form of motion is expressed as (1).

$$[M][\ddot{U}]+[C][\dot{U}]+[K][U]=[F] \quad (1)$$

In the given context, it represents the matrix and $[\ddot{U}]$ is the second time derivative of the displacement $[U]$, corresponding to acceleration. $[\dot{U}]$ represents the velocity, the damping matrix, the stiffness matrix, and the force vector. The quadratic eigenvalue problem arises as a general problem when considering systems with nonzero damping. Nevertheless, the damping is typically disregarded in vibrational modal analysis, excluding all terms except for the first and third terms on the left-hand side, as depicted in (2).

$$[M][\ddot{U}]+[K][U]=[0] \quad (2)$$

The generic form of the eigensystem in structural engineering, as applied in the FEM, can be described as follows. To illustrate the solutions of the free vibrations of the structure, it is hypothesized that the motion adheres to a harmonic pattern. This assumption implies that it is considered equal to, where it represents an eigenvalue denoted in units of reciprocal time squared, such as s^{-2}. By utilizing this approach, the equation can be simplified to (3).

$$[M][U]\lambda+[K][U]=[0] \quad (3)$$

On the other hand, the equation of static problems can be represented as (4). The expected outcome occurs when all terms containing a temporal derivative are equated to zero.

$$[K][U]=[F] \quad (4)$$

Modeling

Figure 1 is the detailed design dimensions of the fan blades with two blades with a blade pitch of 25° drawn using Solidwork. Another design variation is increasing the number of blades to 3

and 4 while the blade pitch varies to 30° and 40°. Previous research analyzed fan performance using variations in blade pitch ranging from 10° to 40° [38]. In this research, we only chose three variations of relatively high values to allow the fan to blow more air. In addition, our focus is analyzing the influence of blade pitch on personal frequency so that the choice of variation values with close intervals is not so influential.

Simulation Process

The analysis in this study uses Solidworks software, utilizing the Solidworks frequency simulation feature. Frequency analysis was done by varying the number of blades 2, 3, and 4 with blade pitch of 25°, 30°, and 40°. After the fan blade design model has been made. The simulation is carried out in the following stages: determining the type of material, deciding the fixed parts, making the mesh, running the analysis, and finally, getting the study results. The type of material used can be seen in Table 1.

They were selected in advance according to the model material used. This study only used one type of material with variations in the number and angle of the same blade, namely PP-Homopolymer. Next, determine the fan blade model section as shown in Figure 2, which is considered a stationary or fixed position. In all variations, the number and angle of blades on the back of the blade face are designated as a fixture.

Meshing Phase

Details of the meshing treatment can be seen in Table 2. The type of mesh used in this study is solid mesh. The mesh density size will affect the accuracy of the analysis results. This study uses a standard-type mesh density with a relatively high accuracy level.

Table 1. Material Property [39][40]

Name	PP-Homopolymer
Model type	Linear elastic isotropic
Tensile strength	3.64+7 N/m^2
Mass density	933 kg/m^3
Elastic modulus	1.8e+9 N/m^2

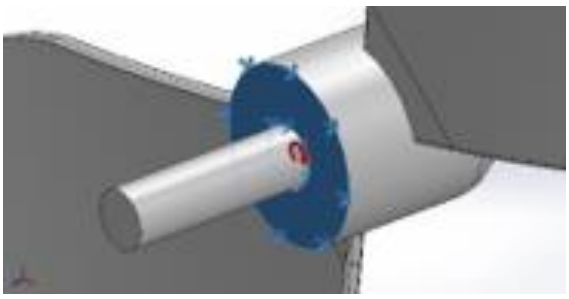

Figure 2. Fixed Part

The following process is to create a mesh on the fan blade model to be analyzed, as shown in Figure 3. This method is used for engineering problems where the exact solution/analytical solution cannot be solved.

The essence of the finite element method is to divide an object to be analyzed into several parts with a limited number. These parts are called elements; each element with one other element is connected with a node (node). The process of dividing objects into parts is called meshing. The type of mesh used in this study is solid mesh, as shown in Table 2. The mesh density size will affect the accuracy of the analysis results. This study uses a standard-type mesh density with a relatively high accuracy level.

The following process is to conduct the running analysis process to get the desired results using the settings and mesh model created earlier. The running process can take different times, depending on the type of mesh density used. The greater the level of mesh density, the longer the running time of the analysis will be due to the higher level of accuracy [24].

Figure 3. Defining Mesh

Table 2. Detail of Mesh

Mesh Type	Solid Mesh
Mesh Used	Standard Mesh
Automatic Transition	Off
Include Mesh Auto Loops	Off
Jacobian points	4 Points
Element Size	9.20114 mm
Tolerance	0.460057 mm
Mesh Quality	High

RESULTS AND DISCUSSION

After carrying out several design and calculation processes discussed in the previous session, starting from determining the type of material, choosing fixtures, and making mesh up to the running process. There were five frequencies for the number of natural frequencies selected in this study. Therefore, five modes of shapes came out. The mode shape is a vibration pattern at the natural frequency of the simulated model image.

The last stage is to get the results of each simulation. For this study, nine simulation results were obtained according to the variation in the number and angle of the blades.

Natural Frequency Simulation Results

The model under consideration exhibits a variance in its design, specifically in the number of blades, which amounts to three. Additionally, the blade pitch of this model is set at an angle of 25°. The results of the simulation are depicted in Figure 4. In addition to acquiring the natural frequency value, the simulation also accepts the consequent amplitude value, which characterizes the movement pattern. The resulting amplitude is the relative displacement value between consecutive points in the frequency analysis. The choice of units will be contingent upon the quantity of the force received, as the simulation does not involve any exertion of power on the fan blades.

The simulation's findings depict the formation of the fan blades, consisting of three blades with a blade pitch of 25°, as illustrated in Figure 4. The description of the resultant amplitude is provided below. (1) The fan blades exhibit a non-reactive vibration at a frequency of 0.0 in blue, indicating a stable and unaffected state. (2) The vibration observed at frequency 2.27 causes a noticeable change in the shape of the fan blades, as indicated by the green color. (3) At a frequency of 4.53 Hz, the vibration experienced by the fan blades is incredibly significant, as represented by the red color. Consequently, it exhibits significant vibrations.

Table 3 presents the natural frequency values corresponding to each mode shape, as derived from the simulation results depicted in Figure 5. The natural frequencies for the first, second, third, fourth, and fifth mode shapes are 22.74, 22.91, 51.92, 52.04, and 76.21 Hz, respectively. However, an identical methodology is employed for the fan category with modifications in the blades' quantity and pitch.

Blades Natural Frequency Analysis

Figure 6 compares the simulation findings for the natural frequency of fan blades. The blades are divided into three groups based on the number of blades, namely two blades, with angles of 25°, 30°, and 40°. The average natural frequency in the first mode shape is 22.68 Hz, whereas the middle natural frequency in the second mode shape is 22.91 Hz. It can be observed that altering the number of blades from 2 while adjusting the blade pitch to 25°, 30°, and 40° in both the first and second modes does not influence the inherent frequency. The third mode has a frequency of 53.3 Hz, the fourth mode has a frequency of 53.42 Hz, and the average natural frequency value in the fifth mode form is 74.11 Hz. Furthermore, it can be observed that altering the number of blades and blade pitch in the third, fourth, and fifth modes has minimal impact on the natural frequency.

Figure 6 illustrates the numerical representation of three blades, each possessing angles of 25°, 30°, and 40°. The average natural frequency in the first mode shape is 22.70 Hz, while the intermediate natural frequency in the second mode is 22.82 Hz. The average natural frequency in the third mode shape is 22.96 Hz. This implies that alterations in the number of blades, in conjunction with adjustments in the blade pitch, do not influence the inherent frequency observed in the first, second, and third mode shapes. Additionally, it should be noted that the average natural frequency value in the fourth mode is 53.56 Hz, whereas in the fifth mode, it is 54.52 Hz. The results indicate that modifying the number of blades and the pitch of the blades in the fifth mode has negligible influence on the inherent frequency.

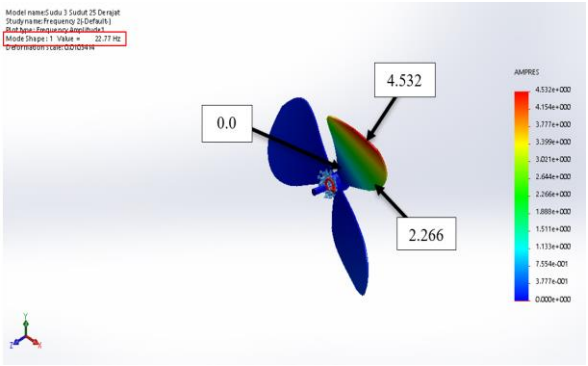

Figure 4. Simulation of 3 blades and pitch 25°

Table 3. Simulation of 3 blades with pitch 25°

Mode Shape	Natural Frequency (Hz)
1	22.77
2	22.858
3	22.941
4	52.146
5	52.759

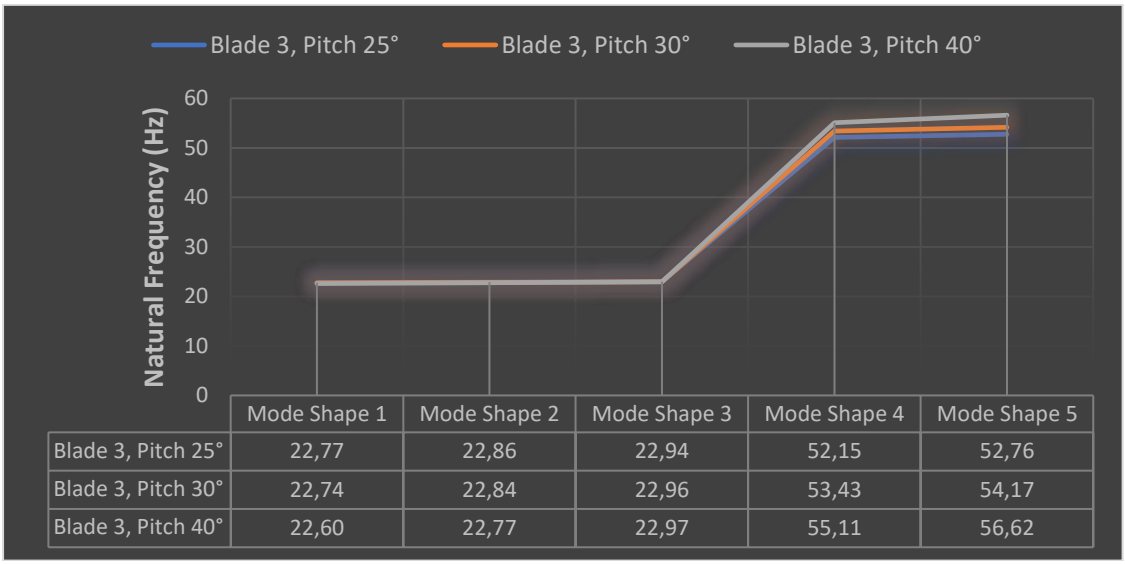

	Mode Shape 1	Mode Shape 2	Mode Shape 3	Mode Shape 4	Mode Shape 5
Blade 3, Pitch 25°	22,77	22,86	22,94	52,15	52,76
Blade 3, Pitch 30°	22,74	22,84	22,96	53,43	54,17
Blade 3, Pitch 40°	22,60	22,77	22,97	55,11	56,62

Figure 5. Natural Frequency Comparison 3 Blades

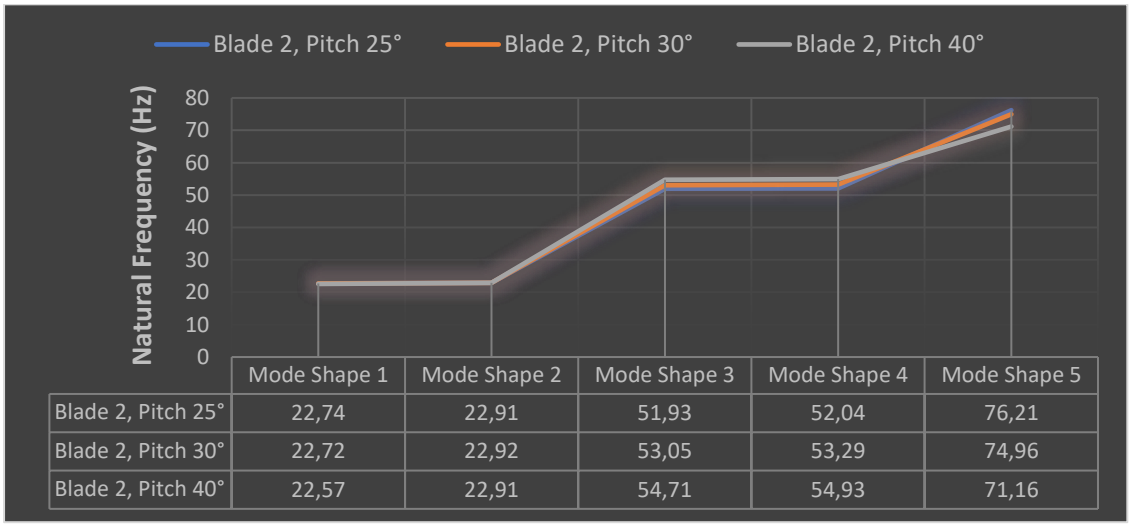

	Mode Shape 1	Mode Shape 2	Mode Shape 3	Mode Shape 4	Mode Shape 5
Blade 2, Pitch 25°	22,74	22,91	51,93	52,04	76,21
Blade 2, Pitch 30°	22,72	22,92	53,05	53,29	74,96
Blade 2, Pitch 40°	22,57	22,91	54,71	54,93	71,16

Figure 6. Natural Frequency Comparison 2 Blades

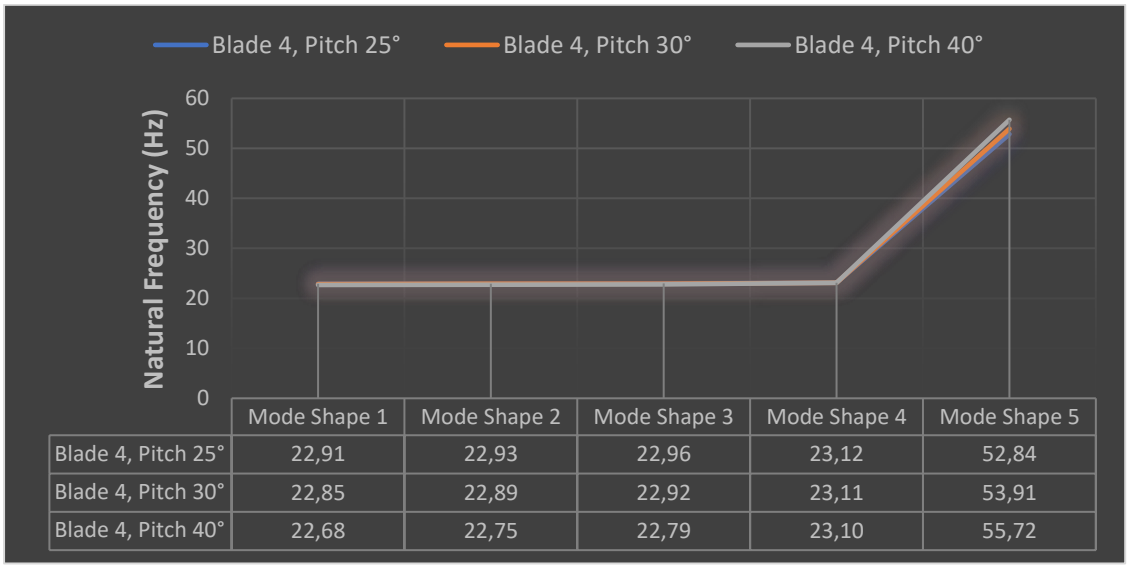

	Mode Shape 1	Mode Shape 2	Mode Shape 3	Mode Shape 4	Mode Shape 5
Blade 4, Pitch 25°	22,91	22,93	22,96	23,12	52,84
Blade 4, Pitch 30°	22,85	22,89	22,92	23,11	53,91
Blade 4, Pitch 40°	22,68	22,75	22,79	23,10	55,72

Figure 5. Comparison of Natural Frequency of 2 Blades and Motor Frequency

Figure 7 shows the number of blades 4 with blade pitch of 25°, 30°, and 40°. In the first mode shape, the average natural frequency value is 22.81 Hz; in the second mode, the average natural frequency value is 22.86 Hz, then in the third mode, the average natural frequency value is 22.888 Hz then in the fourth mode, the average natural frequency is 23.11 Hz. This means that changing the variation of the number of blades with the blade pitch does not affect the natural frequency. And finally, in the fifth mode, the average natural frequency value is 54.06 Hz. This also indicates that changing the number of blades and the blade pitch has little effect on the natural frequency in the fifth mode.

Blades and Motor Frequency Analysis

The motor's rotation speed is adjusted to three different frequencies: 25 Hz, 35 Hz, and 50 Hz. The frequency of the fan blades is then compared and studied concerning the natural frequency of the blades. This analysis aims to determine whether resonance will occur between the fan blades and the motor's rotation frequency. Resonance may arise and pose a risk to the structural integrity of the fan blades if the ratio between the rotational frequency of the motor and the natural frequency of the blades is equivalent or nearly equivalent. Nevertheless, if the values of the two frequencies differ, resonance will not transpire, indicating that the fan blade design is secure. The graph presented in Figures 8, 9, and 10 compares the natural frequency of fan blades. Specifically, the analysis focuses on fan blades with three blades, each having an angle of 25°, 30°, and 40°. The natural frequency of these blades is examined concerning motor rotation frequency.

The data presented in Figure 8 illustrates the motor rotation frequency of 25 Hz. The average natural frequency values for the first and second mode forms are also recorded as 22.68 Hz and 22.91 Hz, respectively. This implies that the mode shapes 1 and 2 exhibit distinct values from the motor rotation frequency of 25 Hz, hence preventing resonance from occurring on the fan blades. In addition, when the motor rotation frequency is set at 35 Hz, the average natural frequency values for the third and fourth mode shapes are determined to be 53.3 Hz and 53.42 Hz, respectively. Additionally, it can be observed that the mode shapes 3 and 4 do not exhibit the same values as the motor rotation frequency of 35 Hz, thereby indicating the absence of resonance in the fan blades. At a motor rotation frequency of 50 Hz, the average natural frequency value in the fifth mode shape is determined to be 74.11 Hz. Consequently, the fifth mode shape does not align with the motor rotation frequency of 50 Hz, thereby precluding resonance on the fan blades. In the absence of information regarding the correlation between the fan blades' frequency and the motor's rotational frequency, we may confidently assert that the fan blades' design is deemed safe.

Figure 9 compares the natural frequencies of fan blades with three blades and varying pitch angles of 25°, 30°, and 40°. The rotational frequency of the motor is 25 Hz, while the average natural frequencies in the first and second mode shapes are 22.70 Hz and 22.82 Hz, respectively. This implies that the mode shapes 1 and 2 exhibit distinct values from the motor rotation frequency of 25 Hz, leading to the absence of resonance on the fan blades.

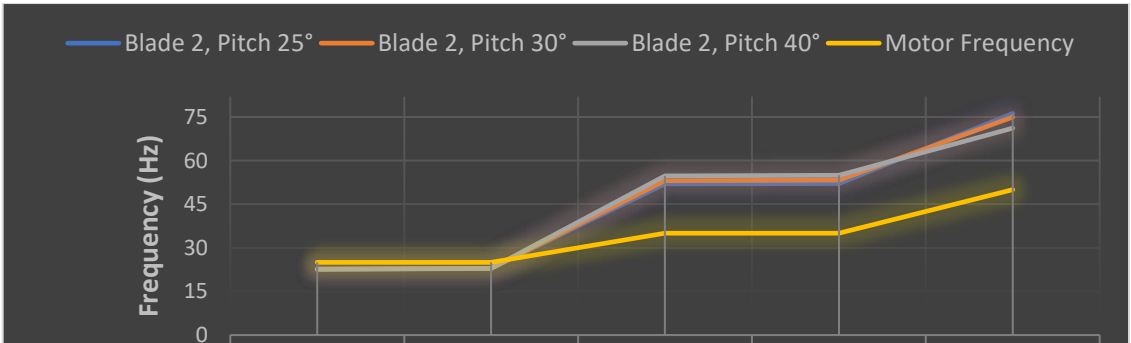

	Mode Shape 1	Mode Shape 2	Mode Shape 3	Mode Shape 4	Mode Shape 5
Blade 2, Pitch 25°	22,74	22,91	51,93	52,04	76,21
Blade 2, Pitch 30°	22,72	22,92	53,05	53,29	74,96
Blade 2, Pitch 40°	22,57	22,91	54,71	54,93	71,16
Motor Frequency	25,00	25,00	35,00	35,00	50,00

Figure 6. Comparison of Natural Frequency of 2 Blades and Motor Frequency

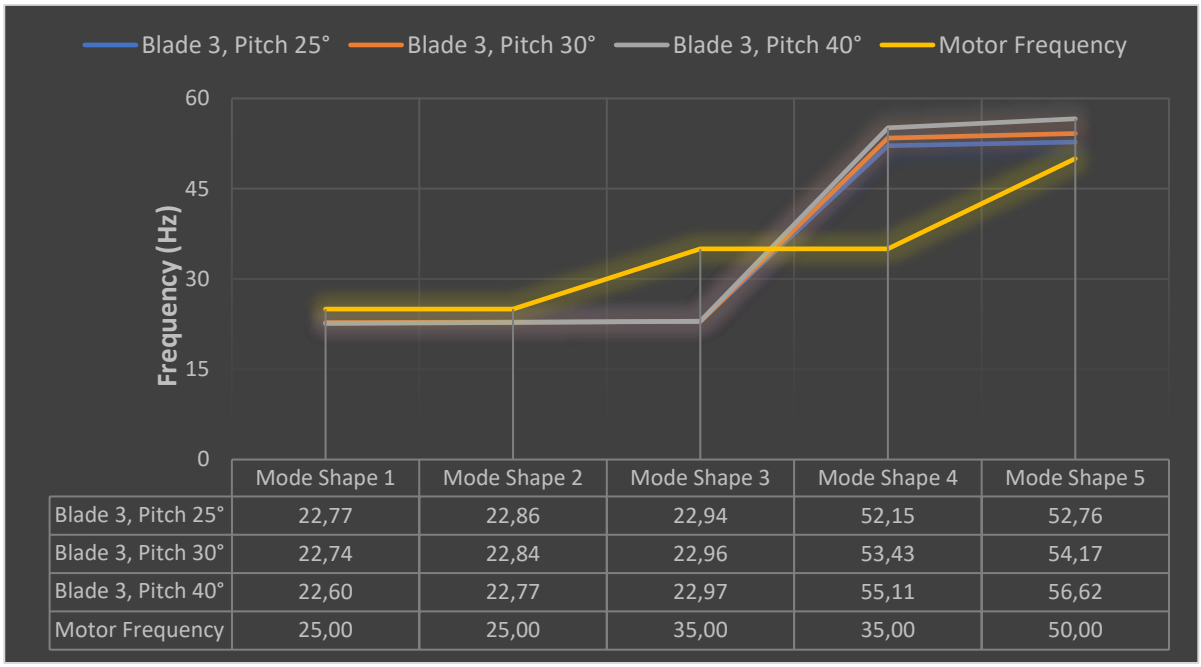

	Mode Shape 1	Mode Shape 2	Mode Shape 3	Mode Shape 4	Mode Shape 5
Blade 3, Pitch 25°	22,77	22,86	22,94	52,15	52,76
Blade 3, Pitch 30°	22,74	22,84	22,96	53,43	54,17
Blade 3, Pitch 40°	22,60	22,77	22,97	55,11	56,62
Motor Frequency	25,00	25,00	35,00	35,00	50,00

Figure 7. Comparison of Natural Frequency of 3 Blades and Motor Frequency

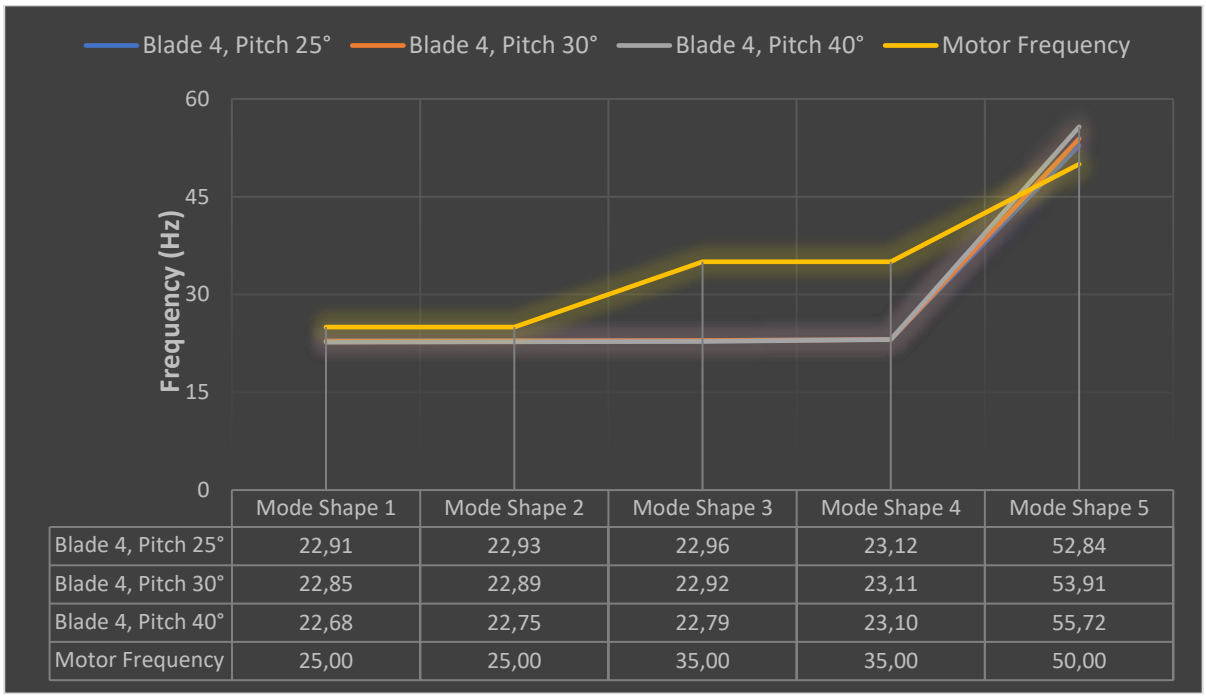

	Mode Shape 1	Mode Shape 2	Mode Shape 3	Mode Shape 4	Mode Shape 5
Blade 4, Pitch 25°	22,91	22,93	22,96	23,12	52,84
Blade 4, Pitch 30°	22,85	22,89	22,92	23,11	53,91
Blade 4, Pitch 40°	22,68	22,75	22,79	23,10	55,72
Motor Frequency	25,00	25,00	35,00	35,00	50,00

Figure 8. Comparison of Natural Frequency of 4 Blades and Motor Frequency

Moreover, when the motor rotation frequency reaches 35 Hz, the average natural frequency in the third mode is measured to be 22.96 Hz, while the fourth mode shape has a frequency of 53.56 Hz. Additionally, it can be observed that the values assigned to mode shapes 3 and 4 do not align with the motor rotation frequency of 35 Hz, leading to the absence of resonance in the fan blades. At a motor rotation frequency of 50 Hz, the average natural frequency value in the fifth mode shape is determined to be 54.52 Hz. Consequently, the fifth mode shape's value does not align with the motor rotation frequency of 50 Hz, thereby preventing resonance from occurring on the fan blades. Without information regarding the alignment between the fan blades' frequency and the motor's rotational frequency, one can assert that the fan blades' design is safe.

Figure 10 presents the natural frequency of fan blades with varying blade configurations, specifically when the number of blades is four and the pitch angles are 25°, 30°, and 40°. The mean value of the natural frequency in the first mode shape is 22.81 Hz, whereas in the second mode, it is 22.86 Hz. This implies that modes 1 and 2 exhibit dissimilarity with the motor rotation frequency of 25 Hz, leading to no resonance on the fan blades. Moreover, when the motor rotation frequency reaches 35 Hz, the average natural frequency values for the third and fourth modes are 22.89 Hz and 23.11 Hz, respectively. Furthermore, it can be observed that the values assigned to forms 3 and 4 do not align with the motor rotation frequency of 35 Hz, hence leading to the absence of resonance in the fan blades. At a motor rotation frequency of 50 Hz, the average natural frequency value in the fifth mode shape is determined to be 54.06 Hz. This implies that the cost of the fifth mode of form is not equivalent to the motor's rotational frequency of 50 Hz, preventing resonance from occurring on the fan blades. In the absence of information regarding the alignment between the fan blades' frequency and the motor's rotational frequency, it can be concluded that the fan blades' design is deemed safe.

All experimental findings yielded similar results. The variations in the number of blades and pitch do not interfere with the motor rotation employed. Upon examining the entirety of the graphical representations illustrating the comparative outcomes, it becomes evident that alterations in the quantities of blades and pitch values do not exert any discernible influence on the natural frequency values of shape modes 1 to 3. Furthermore, their impact on shape modes 4 and 5 is minimal. However, based on the observed pattern, it can be inferred that there is a positive correlation between the changes and the frequency, indicating that as the frequency increases, the changes also tend to increase. Selecting the motor speed is of utmost significance to avoid any potential collision with the inherent frequency of the fan blades. The investigation shows minimal disparity between motor speed and natural frequency. In this scenario, it is imperative to refrain from selecting motor speeds between 22 to 23 Hz and 52 to 56 Hz.

The present study employs a finite element method methodology to ascertain the natural frequency of the fan blade design. The utilization of computational results holds significant importance in mitigating resonance phenomena. A similar approach was also employed by [6]. Their study aimed to design a vertical wind turbine to harness wind energy generated by vehicles in the parking lane. The significant generation of wind energy can be attributed to the differential pressure created by the movement of automobiles on the road. Modal analysis is an integral part of the design process, wherein the CATIA workbench is utilized to ascertain the natural frequency values. The primary objective of this analysis is to mitigate the occurrence of resonance. In addition, the researchers also conducted calculations to determine the design strength of the wind turbine, considering factors such as strain, deformation, and shear pressure. The identical concept is also employed by [7, 15, 16]. The findings of this study indicate that Figures 8 to 10 display the disparities in motor and blade frequency values. Similar findings were observed in prior studies. A higher discrepancy between the values of motor and blade frequencies is associated with improved performance, whereas conversely, a lower discrepancy is associated with poorer performance. Most systems possess a specific operating frequency, and it is crucial to evaluate whether the inherent frequencies of compliant mechanisms fall within this range to guarantee seamless operation. Including a mechanism with a natural frequency proximate to the operational frequency of the overall system might result in resonance, ultimately culminating in malfunction and damage.

CONCLUSION

This study demonstrates obtaining natural fan blade frequencies using SolidWorks software's frequency simulation capability, employing the finite element approach. This involves constructing a fan blade model, inputting relevant fan parameters, generating a mesh, executing the simulation process, and acquiring the corresponding natural frequency values. All experimental experiments yielded similar outcomes. The variations in the number of blades and pitch do not interfere with the motor rotation employed. This implies that the fan blade does not exhibit resonance with the frequency of motor rotation, hence ensuring the safety of this design, as the natural frequency of the fan blade does not align with the magnitude of the motor rotation frequency. Based on the graphical representation of the comparative outcomes, it can be observed that alterations in the number of blades and pitch values do not exert any discernible influence on the natural frequency values within first to third-mode shapes. Furthermore, these modifications exhibit minimal impact on the natural frequency values within fourth and fifth mode shapes. However, based on the observed pattern, it can be inferred that there is a positive correlation between

the magnitude of changes and the frequency of occurrence.

ACKNOWLEDGMENT

The authors sincerely thank Mercu Buana University for its financial support, contract No. 02-5/1348/B-SPK/V/2023.

REFERENCES

[1] F. Anggara, D. Romahadi, A. L. Avicenna, and Y. H. Irawan, "Numerical analysis of the vortex flow effect on the thermal-hydraulic performance of spray dryer," *SINERGI*, vol. 26, no. 1, pp. 23–30, Feb. 2022, doi: 10.22441/sinergi.2022.1.004.

[2] A. A. Luthfie, D. Romahadi, H. Ghufron, and S. D. Murtyas, "Numerical simulation on rear spoiler angle of mini MPV car for conducting stability and safety," *SINERGI*, vol. 24, no. 1, pp. 23–28, Dec. 2019, doi: 10.22441/sinergi.2020.1.004.

[3] D. F. Plöger, P. Zech, and S. Rinderknecht, "Vibration signature analysis of commodity planetary gearboxes," *Mechanical Systems and Signal Processing*, vol. 119, pp. 255–265, Mar. 2019, doi: 10.1016/j.ymssp.2018.09.014.

[4] C. Zhou et al., "Vibration singularity analysis for milling tool condition monitoring," *International Journal of Mechanical Sciences*, vol. 166, p. 105254, Jan. 2020, doi: 10.1016/j.ijmecsci.2019.105254.

[5] D. Romahadi, A. A. Luthfie, and L. B. D. Dorion, "Detecting classifier-coal mill damage using a signal vibration analysis," *SINERGI*, vol. 23, no. 3, pp. 175–183, Sep. 2019, doi: 10.22441/sinergi.2019.3.001.

[6] S. S. Seelamsetti, V. N. P. Darbha, and V. R. Mamilla, "Design and structural analysis using FEM of highway composite helical wind turbine," *Materials Today: Proceedings*, Jun. 2023, doi: 10.1016/j.matpr.2023.06.191.

[7] N. S. Pirogova and P. A. Taranenko, "Calculative and Experimental Analysis of Natural and Critical Frequencies and Mode Shapes of High-speed Rotor for Micro Gas Turbine Plant," *Procedia Engineering*, vol. 129, pp. 997–1004, Jan. 2015, doi: 10.1016/j.proeng.2015.12.162.

[8] K. Vardaan and P. Kumar, "Design, analysis, and optimization of thresher machine flywheel using Solidworks simulation," *Materials Today: Proceedings*, vol. 56, pp. 3651–3655, Jan. 2022, doi: 10.1016/j.matpr.2021.12.348.

[9] R. Mahakul, D. Nath Thatoi, S. Choudhury, and P. Patnaik, "Design and numerical analysis of spur gear using SolidWorks simulation technique," *Materials Today: Proceedings*, vol. 41, pp. 340–346, Jan. 2021, doi: 10.1016/j.matpr.2020.09.554.

[10] R. N. A. Kurniawan, D. Romahadi, M. Fitri, and M. R. Karim, "Implementation of the Finite Element Method in Solidworks to optimize the front cast wheel design for motorcycles," *International Journal of Innovation in Mechanical Engineering & Advanced Materials (IJIMEAM)*, vol. 4, no. 3, pp. 66–73, 2023, doi: 10.22441/ijimeam.v4i3.18794.

[11] M. Holst and M. Licht, "Geometric transformation of finite element methods: Theory and applications," *Applied Numerical Mathematics*, vol. 192, pp. 389–413, Oct. 2023, doi: 10.1016/j.apnum.2023.07.002.

[12] C. Lee and J. Park, "Preconditioning for finite element methods with strain smoothing," *Computers & Mathematics with Applications*, vol. 130, pp. 41–57, Jan. 2023, doi: 10.1016/*J.CAMWA*.2022.11.018.

[13] X. Wang, X. Meng, S. Zhang, and H. Zhou, "A modified weak Galerkin finite element method for the linear elasticity problem in mixed form," *Journal of Computational and Applied Mathematics*, vol. 420, p. 114743, Mar. 2023, doi: 10.1016/j.cam.2022.114743.

[14] I. Tomoyuki, N. Yuto, T. Nobukazu, and T. Masaki, "The modeling and analysis for the natural frequency adjustments of Vehicle Manipulator for the ITER Blanket Remote Handling System," *Fusion Engineering and Design*, vol. 192, p. 113802, Jul. 2023, doi: 10.1016/j.fusengdes.2023.113802.

[15] J. Sánchez-Haro, I. Lombillo, and G. Capellán, "Modelling criteria proposal for dynamic analysis of beam bridges under moving loads using fem models," *Structures*, vol. 50, pp. 651–669, Apr. 2023, doi: 10.1016/j.istruc.2023.02.067.

[16] V. Platl and L. Zentner, "An analytical method for calculating the natural frequencies of spatial compliant mechanisms," *Mechanism and Machine Theory*, vol. 175, p. 104939, Sep. 2022, doi: 10.1016/j.mechmachtheory.2022.104939.

[17] Z. Liu et al., "Traveling wave resonance analysis of flexible spur gear system with angular misalignment," *International Journal of Mechanical Sciences*, vol. 232, p. 107617, Oct. 2022, doi: 10.1016/j.ijmecsci.2022.107617.

[18] H. Li, W. Yang, P. Liu, and M. Wang, "Resonance measurement and vibration reduction analysis of an office building induced by nearby crane workshop vibration," *Journal of Building Engineering*, vol. 58, p.

105018, Oct. 2022, doi: 10.1016/j.jobe.2022.105018.
[19] J. Qi, M. Miyashita, T. Ogawa, H. Naito, and K. Sasaki, “Resonance frequency analysis for evaluation of the connecting condition between fixed prostheses and their abutment teeth: An in vitro and finite element analysis study,” *Journal of Prosthetic Dentistry*, Apr. 2022, doi: 10.1016/j.prosdent.2022.03.005.
[20] L. Xin, D. Mu, D. H. Choi, X. Li, and F. Wang, “General conditions for the resonance and cancellation of railway bridges under moving train loads,” *Mechanical Systems and Signal Processing*, vol. 183, p. 109589, Jan. 2023, doi: 10.1016/j.ymssp.2022.109589.
[21] J. Li, H. Zhang, D. Zhu, and C. Li, “A moving load amplitude spectrum for analyzing the resonance and vibration cancellation of simply supported bridges under moving loads,” *European Journal of Mechanics - A/Solids*, vol. 92, p. 104428, Mar. 2022, doi: 10.1016/j.euromechsol.2021.104428.
[22] J. Qi, M. Miyashita, T. Ogawa, H. Naito, and K. Sasaki, “Resonance frequency analysis for evaluation of the connecting condition between fixed prostheses and their abutment teeth: An in vitro and finite element analysis study,” *Journal of Prosthetic Dentistry*, Apr. 2022, doi: 10.1016/j.prosdent.2022.03.005.
[23] H. Huang and C. Wang, “Finite element simulations of second order wave resonance by motions of two bodies in a steady current,” *Ocean Engineering*, vol. 196, p. 106734, Jan. 2020, doi: 10.1016/j.oceaneng.2019.106734.
[24] S. Yang et al., “Stress and strain changes of the anterior cruciate ligament at different knee flexion angles: A three-dimensional finite element study,” *Journal of Orthopaedic Science*, Jul. 2023, doi: 10.1016/j.jos.2023.05.015.
[25] L. Zhao, X. Yang, J. Wang, Y. Chai, Y. Li, and C. Wang, “Improved frequency-domain Spectral Element Method for vibration analysis of nonuniform pipe conveying fluid,” *Thin-Walled Structures*, vol. 182, p. 110254, Jan. 2023, doi: 10.1016/j.tws.2022.110254.
[26] A. A. F. Ogaili, A. Abdulhady Jaber, and M. N. Hamzah, “Wind turbine blades fault diagnosis based on vibration dataset analysis,” *Data Brief*, vol. 49, p. 109414, Aug. 2023, doi: 10.1016/j.dib.2023.109414.
[27] W. Liu, Z. Guan, S. Zhang, and Y. Li, “Numerical and experimental investigation on autoparametric resonance of multi-system structures,” *International Journal of Mechanical Sciences*, vol. 259, p. 108591, Dec. 2023, doi: 10.1016/j.ijmecsci.2023.108591.
[28] Q. Guan, B. Liu, Z. Wen, and X. Jin, “Analysis of the resonance frequencies of multiple wheels–track coupled system based on the wave approach,” *Journal of Sound and Vibration*, vol. 568, p. 117956, Jan. 2024, doi: 10.1016/j.jsv.2023.117956.
[29] F. Wang, T. Sasamura, Y. Jiang, S. Miyake, J. Twiefel, and T. Morita, “Dynamic resonance frequency control for a resonant-type smooth impact drive mechanism actuator,” *Sensors and Actuators A: Physical*, vol. 359, Sep. 2023, doi: 10.1016/j.sna.2023.114462.
[30] Y. Yang, S. Li, A. Song, Y. Luo, H. Fang, and Y. Feng, “Impedance-frequency characteristic analysis of bypass damping filter in suppressing AC–DC system’s subsynchronous resonance,” *Energy Reports*, vol. 9, pp. 36–48, Sep. 2023, doi: 10.1016/j.egyr.2023.04.084.
[31] H. Li, W. Yang, P. Liu, and M. Wang, “Resonance measurement and vibration reduction analysis of an office building induced by nearby crane workshop vibration,” *Journal of Building Engineering*, vol. 58, p. 105018, Oct. 2022, doi: 10.1016/j.jobe.2022.105018.
[32] B. Yan et al., “Experimental study on the aeroelastic response of a square supertall building considering twisted wind effect,” *Engineering Structures*, vol. 283, May 2023, doi: 10.1016/j.engstruct.2023.115923.
[33] S. Chen, Q. Liu, C. Zhai, and W. Wen, “Influence of building-site resonance and building properties on site-city interaction: A numerical investigation,” *Soil Dynamics and Earthquake Engineering*, vol. 158, Jul. 2022, doi: 10.1016/j.soildyn.2022.107307.
[34] M. Gu, L. Su, Y. Quan, J. Huang, and G. Fu, “Experimental study on wind-induced vibration and aerodynamic mitigation measures of a building over 800 meters,” *Journal of Building Engineering*, vol. 46, p. 103681, Apr. 2022, doi: 10.1016/j.jobe.2021.103681.
[35] L. Dun-xiang, N. Rong-gen, and R. D. Adams, “The finite element technique for predicting the natural frequencies, mode shapes and damping values of filamentary composite plates,” *Applied Mathematics and Mechanics*, vol. 7, no. 2, pp. 197–213, Feb. 1986, doi: 10.1007/BF01897064.
[36] I. Ramu and S. C. Mohanty, “Modal Analysis of Functionally Graded Material Plates Using Finite Element Method,” *Procedia Materials Science*, vol. 6, pp. 460–467, Jan. 2014, doi: 10.1016/j.mspro.2014.07.059.

[37] D. A. Sastranegara, K. E. Putra, E. Halawa, N. A. Sutisna, A. Topa, "Finite Element Analysis on ballistic impact performance of multi-layered bulletproof vest impacted by 9 mm bullet," *SINERGI*, vol. 27, no. 1, pp. 15-22, 2023, doi: 10.22441/sinergi.2023.1.003.
[38] D. Khalitov, R. Ganesh, "Analytical models for axial fan performance," *AMCA Engineering Conference*, Las vegas, USA, March 2008, pp. 1–13.
[39] J. Jancar, A. Dianselmo, and A. T. Dibenedetto, "The yield strength of particulate reinforced thermoplastic composites," *Polymer Engineering & Science*, vol. 32, no. 18, pp. 1394–1399, 1992, doi: 10.1002/pen.760321809.
[40] G. Rineksa, Y. Whulanza, M. Gozan, "Preliminary Study of Potential Bioimplant from Glycerol Plasticized Starch-Microcrystalline Cellulose Composite," *Journal of Integrated and Advanced Engineering (JIAE)*, vol. 1, no. 1, pp. 29-36, 2021, doi: 10.51662/jiae.v1i1.10